nature portfolio

Peer Review File

Revealing and Modulating Catalyst Reconstruction for Highly Efficient Electrosynthesis of Ammonia

Corresponding Author: Professor Hongfei Cheng

This file contains all reviewer reports in order by version, followed by all author rebuttals in order by version.

Version 0:

Reviewer comments:

Reviewer #1

(Remarks to the Author)
This study presents the synthesis, characterization, and performance investigation of Co6Ni4 heterostructure as an electrocatalyst for NO3RR. The authors used operando X-ray absorption spectroscopy, in-situ characterization techniques and DFT calculations to study the dynamic change of the catalyst and reaction mechanism of the NO3RR. However, this manuscript does not exhibit sufficient novelty in terms of catalyst characteristics and reaction mechanisms, and significant performance advancement. Given these concerns, this manuscript is not recommended for publication in this journal. Some comments are as follows:

1. The present experimental evidence is insufficient to conclusively demonstrate that Co6Ni4 is constituted of randomly interlaced Co and Ni nanodomains. To further confirm the structure of this catalyst, atomic-level resolution STEM-EDS mapping is required.
2. The TEM characterizations revealed that amorphous Co domains were existed in the Co6Ni4 catalyst. However, the effect of amorphous phase or amorphous/crystalline interface on the NO3RR performance is not discussed in the manuscript.
3. Achieving high NH3 Faraday efficiency and yield rate under high NO3- concentrations is not surprising. In practice, the NO3- concentration in most nitrate sources is typically very low (1 to 100 mM). How about the NO3RR performance of Co6Ni4 catalyst in the lower NO3- concentrations (such as 1 and 10 mM).
4. The comparison of performance obtained under different NO3- concentrations is meaningless.
5. The enhanced NO3RR performance of Co6Ni4 catalyst may be attributed to its larger electrochemically active area. To better understand the origin of the high NO3RR performance of Co6Ni4, the intrinsic activity of Co6Ni4 catalyst should be investigated and compared with Co and Ni catalysts.

Reviewer #2

(Remarks to the Author)
This paper presents a well-executed and interesting study on the possible structure reconstruction phenomenon of Co-based catalysts toward electrocatalytic nitrate reduction reaction (NO3RR). Co6Ni4 heterostructured materials as a model catalyst was developed, and suggested with high NO3RR activity, even under industrially ampere current conditions. The improved performance and stable structure arise from the electron communication with Ni and Co domains in Co6Ni4, where the Ni domains transfer electrons to Co and prevent the accumulation of high-valence Co. The manuscript is well-structured, logically coherent, and presents a comprehensive combination of electrochemical analysis, in-situ/ex-situ material characterization to support the conclusions. The work is of high relevance to the field of nitrate reduction reaction for ammonia production and will be valuable for both fundamental research and industrial applications. Therefore, I recommend acceptance after addressing the following issues:

1. When deciphering the structure ordering within Co6Ni4 catalyst, author used the relative intensity of metal-metal scattering path to explain the atomic ordering of Co and Ni. Author should use this description with great caution, as the synchrotron radiation data does not sufficiently support the related conclusion. Otherwise, references must be cited in relevant part.
2. The electron transfer Ni domains to Co was the key point to prevent the accumulation of high-valence Co, that was proved by XPS and XAS. This phenomenon was also associated with oxidative state increase on Ni site, and valence state of Co,

which seems in contradictory of XAS result, as the metallic state dominate the Co6Ni4 compositions. More explanation shall provide on this part.
3. The Co6Ni4 consisted of abundant amorphous and crystalline part, the exact role of those heterostructure was not well illustrated for the structure-activity relationship.
4. How does the interaction between Ni and Co domains in Co6Ni4? Without any bond bridge within them, the electron transfer remains impossible. More concise discussion have to include for a better understanding of current work.

Reviewer #3

(Remarks to the Author)
In this study, the authors synthesized a series of CoxNiy heterostructured catalysts to investigate the reconstruction behavior of metallic Co during NO3RR. By combining operando XAS, in-situ Raman spectroscopy, and other characterization methods, they identified that the oxidation state evolution of Co arises from an imbalance between the catalyst's electron transfer capacity and the electron demand for adsorbed NO3- reduction. The Co6Ni4 catalyst achieves a high FE and high yield rate for NH3 production, as well as excellent stability. This work elucidates the origin of metallic Co reconstruction during NO3RR and proposes rational regulation strategies, offering critical insights for future catalyst design. The findings are impactful, and I recommend it for publication after a minor revision.
1. The introduction states that NO3RR typically exhibits higher NH3 yield in alkaline environments compared to neutral conditions. Does this trend hold for Co6Ni4? A direct comparison of NH3 FE and yield in neutral vs. alkaline electrolytes would clarify this claim.
2. In Figure S11, the current density in the first cycle is notably lower than in subsequent cycles. What causes this discrepancy?
3. At OCP, Co catalyst is oxidized to a higher valence state (Figures 3a and c), which suggests that the spontaneous reduction reaction of NO3- may occur. What are the products of this spontaneous NO3- reduction reaction? Does this interfere with NH3 quantification or FE calculations?
4. The MEA employs a proton-exchange membrane rather than an anion-exchange membrane. What is the rationale for this choice?
5. Figure S13 and S14 reveal slight morphology change of Co6Ni4 after stability tests. The corresponding description in the manuscript needs to be revised.
6. The manuscript repeatedly mentions that the performance of NO3RR declines when the Co catalyst is oxidized to a higher valence state. Could the authors provide direct evidence to support this claim?

Version 1:

Reviewer comments:

Reviewer #1

(Remarks to the Author)
The authors have addressed the comments,and there is no further comments for this manuscript.

Reviewer #2

(Remarks to the Author)
The authors addressed all the reviewers' concerns, and thus it seems now ready for publication.

Reviewer #3

(Remarks to the Author)
The authors have revised the manuscript according to the reviewers's comments, the manuscript could be accepted at current version.

Manuscript Number: NCOMMS-25-11348

Article Type: Research Article

Title: Revealing and Modulating Catalyst Reconstruction for Highly Efficient Electrosynthesis of Ammonia

A Point-by-Point Response to Reviewers' Comments

Dear Editor and Reviewers,

We sincerely appreciate the careful review of our manuscript and the constructive feedback provided. The comments have been invaluable in enhancing the quality of this work. We have addressed all concerns raised by the reviewers, and the corresponding revisions are highlighted in yellow in the revised manuscript and supporting information. A point-by-point response to reviewers' comments is provide below.

Reviewer #1: This study presents the synthesis, characterization, and performance investigation of Co_6Ni_4 heterostructure as an electrocatalyst for NO_3RR. The authors used operando X-ray absorption spectroscopy, in-situ characterization techniques and DFT calculations to study the dynamic change of the catalyst and reaction mechanism of the NO_3RR. However, this manuscript does not exhibit sufficient novelty in terms of catalyst characteristics and reaction mechanisms, and significant performance advancement. Given these concerns, this manuscript is not recommended for publication in this journal. Some comments are as follows:

Response: We would like to express our gratitude for your review and guidance on our work. In response to your concerns on the novelty, we will address them from three key aspects, including catalyst design, reaction mechanism, and performance optimization. Firstly, from the aspect of catalyst design, Co metal is widely used in nitrate reduction (NO_3RR) due to its activity. However, it undergoes significant structural reconstruction during NO_3RR, partially converting to $Co(OH)_2$. The accumulation of low-activity $Co(OH)_2$ leads to performance degradation. To address this, we synthesized a Co catalyst and identified that the mismatch between adsorbed NO_3^- quantity and electron availability on its surface drives reconstruction. To suppress high-valent cobalt

formation, we designed catalysts by reducing NO_3^- adsorption on Co sites and enhancing electron transfer capability. Considering cost constraints, we have selected Fe, Ni, and Cu from the commonly studied elements of NO_3RR for further investigation. Cu is prone to poisoning under high NO_3^- concentrations, making it unsuitable for industrial-scale NH_3 production via NO_3RR with ampere-level current density. Metallic Fe exhibits unsatisfactory NO_3RR activity, while Ni shares similar atomic radius and physicochemical properties with Co, enabling heterostructure formation. Ni also has prior ampere-level NO_3RR research. Thus, we designed a Co_6Ni_4 heterostructured catalyst by incorporating Ni nanocrystals into metallic Co.

Secondly, from the aspect of reaction mechanism, we find that the discrepancy between the adsorption quantity of NO_3^- on catalyst surface and the corresponding electron supply is a pivotal factor influencing the catalyst reconstruction process. Furthermore, we stabilize the metallic Co in the Co_6Ni_4 heterostructured catalyst and achieve its high activity by regulating the electronic interactions between Co and Ni domains, improving electron transport capability, and modulating the adsorption of reaction intermediates. Through operando XAS and in-situ Raman spectroscopy, we confirmed that incorporating Ni nanocrystals effectively suppresses the transformation of metallic Co into $Co(OH)_2$. In-situ EIS and conductivity tests revealed enhanced electron transfer capability in the Co_6Ni_4 catalyst compared to Co catalyst. Additionally, in-situ ATR-FTIR and electrochemical analyses demonstrated that Co and Ni sites preferentially adsorb NO_2^- and NO_3^-, respectively, avoiding excessive NO_3^- adsorption on Co and inhibiting high-valent cobalt accumulation. This tandem mechanism, where distinct sites adsorb different intermediates, further improves NO_3RR performance. Additionally, the combination of XAS and XPS with theoretical calculations reveals that the electron cloud center between Ni and Co shifts towards Co, rendering the Co in an electron-rich state. This also demonstrates that the introduction of Ni enhances the electron transport capability of the catalyst. These findings collectively demonstrate that Ni nanocrystals regulate Co reconstruction and prevent high-valent Co formation.

Lastly, from the aspect of performance advancement, our Co_6Ni_4 catalyst surpasses most of the reported catalysts under similar conditions and is among the top ones. Specifically, in 0.3 M KNO_3 + 1.0 M KOH electrolyte, Co_6Ni_4 achieves >90% Faradaic efficiency (FE) for NH_3 generation across a broad potential range (-0.176 to -0.576 V vs. RHE), peaking at 99.21% FE_{NH_3} (-0.476 V) with an NH_3 yield rate of 93.55 mg h^{-1} cm^{-2}. It operates stably for 120 h at ampere-level current densities and requires only 275 mV overpotential to reach 1 A cm^{-2}. The above performance far surpasses that of

catalysts reported in recent years under the same pH environment and at similar or even higher NO_3^- concentrations (detailed comparisons are provided in Supplementary Table 2).

In summary, we believe this work contributes meaningfully to the field of electrocatalytic nitrate reduction to produce ammonia and respectfully request your reconsideration. Below are our point-by-point responses to your concerns:

Comment 1. The present experimental evidence is insufficient to conclusively demonstrate that Co_6Ni_4 is constituted of randomly interlaced Co and Ni nanodomains. To further confirm the structure of this catalyst, atomic-level resolution STEM-EDS mapping is required.

Response: We appreciate your valuable suggestion. Atomic-scale STEM-EDS mapping would indeed intuitively reveal the distribution of Co and Ni regions in Co_6Ni_4. However, obtaining atomic-scale elemental distribution via STEM-EDS mapping faces significant challenges, such as the strong ferromagnetism of the metallic Co_6Ni_4 catalyst, the close atomic numbers of Co and Ni (resulting in close characteristic X-ray energies), the relatively large size of Co and Ni domains (on the scale of tens of nanometers), and the significantly varied thickness of Co_6Ni_4 structure across different areas. These factors hindered the perfect focusing of electron beam and thus make it hard to obtain an atomic-resolution STEM-EDS mapping.

In view of this, we performed spherical aberration-corrected HAADF-STEM (AC-HAADF-STEM) and the corresponding EDS mapping to reveal the uneven distribution of Co and Ni elements. The AC-HAADF-STEM images (Supplementary Fig. 5) demonstrate that the Co regions in Co_6Ni_4 comprise hcp and amorphous phases, while the Ni regions adopt an fcc phase, which is consistent with the HRTEM images (Fig. 1b-d) and SAED results (Fig. 1a) in the manuscript. The AC-HAADF-STEM-EDS mappings reveal the heterogeneous distribution of Co and Ni elements (Fig. 1f). We believe these findings, combined XRD results (Supplementary Fig. 2) and EDS line scanning (Fig. 1e) in the manuscript, sufficiently elucidate the Co_6Ni_4 is composed of irregular Co and Ni domains.

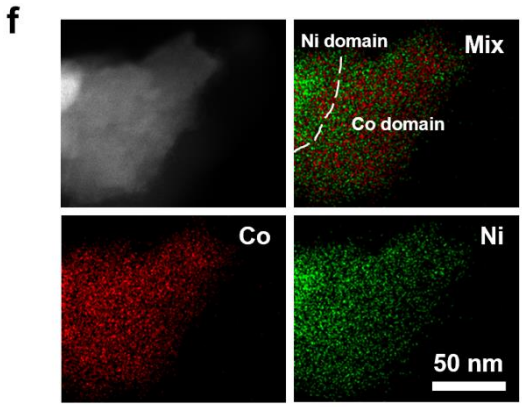

Figure 1. Structural characterizations and of Co_6Ni_4 (f) AC-HAADF-STEM image and the corresponding elemental mappings of Co_6Ni_4.

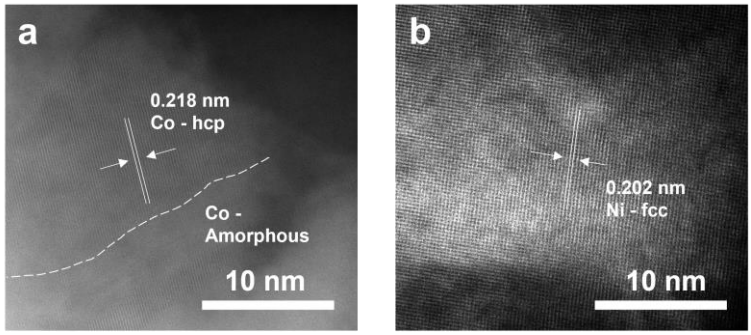

Supplementary Figure 5. (a, b) AC-HAADF-STEM images of Co_6Ni_4.

Corresponding Revision (Page 4):

However, the distribution of Ni and Co elements is uneven on the nanoscale, as evidenced by the EDS linear scanning analysis (**Fig. 1e**), indicating the formation of heterostructure. Furthermore, the interlaced distribution of Co and Ni domains in Co_6Ni_4 was further confirmed by aberration-corrected (AC) HAADF-STEM images (**Supplementary Fig. 5**) and corresponding EDS elemental mapping (**Fig. 1f**). The aforementioned characterization techniques corroborate the assertion that Co_6Ni_4 is a heterostructured catalyst composed of hcp/amorphous Co domains and fcc Ni nanocrystalline domains.

Comment 2. The TEM characterizations revealed that amorphous Co domains were existed in the Co_6Ni_4 catalyst. However, the effect of amorphous phase or amorphous/crystalline interface on the NO_3RR performance is not discussed in the manuscript.

Response: Thanks for raising up this valuable question. To investigate the influence of amorphous phase or amorphous/crystalline interface on the NO_3RR performance, we synthesized the high-crystallinity Co catalyst (Hc-Co). TEM and SAED results demonstrate its high crystallinity (Fig. R1a-d). The Co catalyst in the manuscript has low crystallinity (containing amorphous phase), thus it is denoted as Lc-Co in the subsequent discussion.

The NO_3RR performance evaluation reveals that the Lc-Co exhibits a significantly positive shift in the onset potential compared to the Hc-Co, indicating enhanced NO_3^- adsorption facilitated by the amorphous phase, which aligns with its superior current response (Fig. R2a). The Hc-Co and Lc-Co catalysts shows comparable FE_{NH_3} (Fig. R2b), and the Lc-Co catalyst exhibiting marginally higher FE values only at -0.076 V and -0.176 V. This suggests that the amorphous phase exerts minimal impact on FE_{NH_3}. The ammonia yield of Lc-Co catalyst is higher than that of Hc-Co (Fig. R2c), consistent with its enhanced reduction current in Fig. R2a.

It is worth noting that, the pure Co catalyst and the Co component in in Co_6Ni_4 catalyst both have very poor crystallinity, which eliminates the effect of crystallinity and ensures valid performance comparison and mechanistic analysis of NO_3RR in this work. Therefore, in our work, we focus on the effect of catalyst composition instead of crystallinity. Nevertheless, the effect of amorphous phase or amorphous/crystalline interface on the NO_3RR performance deserves more systematic study and we will study it further in the future work.

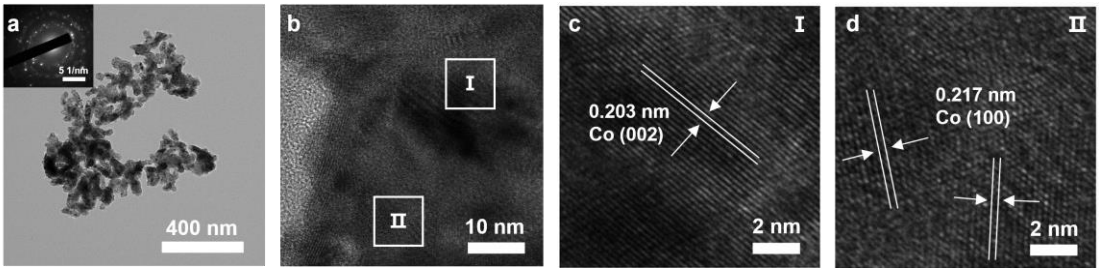

Figure R1. (a) TEM image and SAED pattern, (b-d) HR-TEM images of Hc-Co. Figures (d) and (e) correspond to regions I and II in figure (c), respectively.

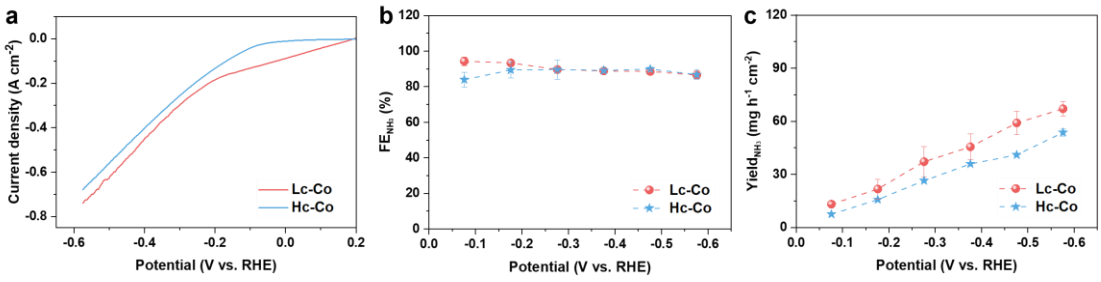

Figure R2. (a) LSV curves, (b) FE, and (c) yield rate of NH_3 of Lc-Co and Hc-Co.

Synthesis of high-crystallinity Co (Hc-Co): Firstly, we prepared $Co(OH)_2$ using an electrodeposition method. The electrode selection and pretreatment of carbon paper followed the same procedures as described in the manuscript. The deposition electrolyte consisted of 30 mL of 0.5 M $Co(NO_3)_2$ aqueous solution, and electrodeposition was carried out at a constant current density of 10 mA cm^{-2} for 600 s. After deposition, the catalyst was thoroughly rinsed with pure water and dried in an oven at 60 °C to obtain $Co(OH)_2$. Subsequently, the $Co(OH)_2$ was annealed in a mixed Ar/H_2 (5%) atmosphere at 400 °C for 3 h, with a heating rate of 5 °C min^{-1}. The hcp-Co catalyst with high crystallinity was obtained after natural cooling.

Comment 3. Achieving high NH_3 Faraday efficiency and yield rate under high NO_3^- concentrations is not surprising. In practice, the NO_3^- concentration in most nitrate sources is typically very low (1 to 100 mM). How about the NO_3RR performance of Co_6Ni_4 catalyst in the lower NO_3^- concentrations (such as 1 and 10 mM).

Response: Thank you for raising up this critical question. The primary objective of this work is to achieve efficient NH_3 synthesis at ampere-level current densities, aiming to replace the energy-intensive and carbon-heavy Haber-Bosch process and advance ammonia-based energy solutions. As you noted, the extremely low NO_3^- concentration in actual wastewater (< 10 mM, *Joule* 2021, 5, 290–294) imposes mass transport limitations, making industrial-scale NH_3 production via NO_3RR nearly impossible. Thus, we evaluated catalyst performance at NO_3^- concentrations exceeding 0.1 M.

NH_3 synthesis from wastewater NO_3^- can only serve as a remediation strategy for human-induced nitrogen cycle disruption, not a replacement for Haber-Bosch-derived NH_3. Recent advances, such as plasma-driven and microbubble-enabled NO_3^- synthesis using air as a feedstock (mentioned in our Introduction), may enable large-scale NO_3^- production to meet the high-concentration demands of industrial NO_3RR. Additionally, nuclear wastewater and certain concentrated industrial effluents (NO_3^- > 0.1 M) could serve as viable high-concentration NO_3^- sources for NO_3RR-based NH_3 synthesis.

The high concentration of NO_3^- alleviates mass transfer limitations, which is beneficial for achieving ampere-level NO_3RR current densities. However, simultaneous attaining high FE and yield rates for NH_3 remains challenging. Copper-based catalysts widely used for NO_3^- removal in wastewater typically exhibit excessively strong NO_3^-

adsorption, leading to catalyst poisoning and subsequent activity degradation. Additionally, their insufficient ability to dissociate water to generate active hydrogen species hinders the reduction of NO_3RR intermediates, resulting in significant NO_2^- accumulation. Therefore, in NO_3RR systems with high NO_3^- concentrations, balancing the NO_3^- adsorption capacity and the ability to dissociate water to generate active hydrogen species is key to achieving superior NO_3RR performance.

In this work, we constructed a heterostructured catalyst using metallic Ni and Co, which exhibits moderate NO_3^- adsorption strength and water dissociation capability. By leveraging the preferential adsorption tendencies of Ni and Co toward NO_3^- and NO_2^-, respectively, we enabled highly efficient tandem NO_3RR processes. This strategy endowed the Co_6Ni_4 catalyst with superior NO_3RR performance. The Co_6Ni_4 catalyst demonstrated competitive performance at 0.3 M NO_3^-, outperforming recently reported catalysts tested at high NO_3^- concentrations (> 0.1 M) and even surpassing most catalysts evaluated at NO_3^- concentrations exceeding 0.3 M (see our response to Comment 4 for details).

We also tested the NO_3RR performance of Co_6Ni_4 in the lower NO_3^- concentrations, i.e., 10 mM and 1 mM. LSV curves confirmed a current density response to NO_3^- addition, indicating catalytic activity towards NO_3RR (Fig. R3a). However, as shown in Fig. R3b and c, the maximum FE_{NH_3} at 1 mM and 10 mM NO_3^- was low (64.11% and 20.26%, respectively), and the corresponding NH_3 yield rates are 2.64 mg h^{-1} cm^{-2} and 0.36 mg h^{-1} cm^{-2}, respectively. These results confirm that this catalyst is unsuitable for wastewater NO_3^- removal.

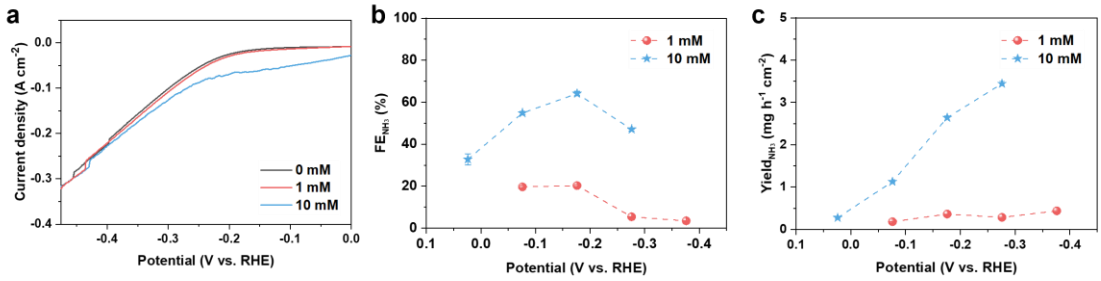

Figure R3. (a) LSV curves of Co_6Ni_4 for NO_3RR in different NO_3^- concentrations. (b) FE and (c) yield rate of NH_3 for Co_6Ni_4 in 1 mM and 10 Mm NO_3^- concentrations at applied potentials.

Comment 4. The comparison of performance obtained under different NO_3^- concentrations is meaningless.

Response: Thank you for raising up this valuable comment. Through reviewing the literatures regarding electrocatalytic NO_3RR, it can be found that the optimal NO_3^- concentration for catalysts to achieve peak NO_3RR performance varies due to their different NO_3^- adsorption capacities and different abilities to generate active hydrogen through water dissociation. At higher NO_3^- concentrations, mass transfer of NO_3^- is not a rate-limiting step, which is beneficial for generating greater current densities; however, the intensive NO_3^- adsorption at higher NO_3^- concentrations will also compete with water dissociation for active hydrogen generation, which may hinder the hydrogenation reaction of NO_3^- and eventually lead to a lower FE of NH_3. Therefore, comparing the peak NO_3RR performance of catalysts at similar NO_3^- concentrations is acceptable in the literatures. Given our research objective of enabling industrial-scale ammonia production via NO_3RR, we specifically focused on comparing catalyst performance at elevated concentrations (> 0.1 M). It is worth emphasizing that in our comparative analysis, more than half of the reference catalysts were tested at NO_3^- concentrations exceeding our selected 0.3 M.

The Co_6Ni_4 catalyst demonstrates exceptional performance at 0.3 M NO_3^- concentration, maintaining competitive advantages even when compared to systems employing 0.5 M or 1.0 M NO_3^- concentrations (**Supplementary Table 2**). Our comparative methodology aligns with parameter selection criteria widely adopted in recent publications, ensuring scientific validity and consistency with established research practices in this field (*J. Am. Chem. Soc.* 2024, 146, 27417–27428; *Adv. Mater.* 2024, 36, 2405660; *Nat. Commun.* 2024, 15, 3619).

Supplementary Table 2. Comparison of the NO_3RR performance of recently reported electrocatalysts.

Catalyst	Potential @ 1A cm^{-2} (V vs. RHE)	E (V vs. RHE)	FE_{NH3} (%)	$Yield_{NH3}$ ($mg\ h^{-1}\ cm^{-2}$)	Stability (h)	Electrolyte	Ref.
Co_6Ni_4	-0.276	-0.476	99.21	93.55	120	0.3 M KNO_3 + 1 M KOH	This work
NiCoP	-0.48 100% iR	-0.3 100% iR	99.7	55.33	24	1.0 M KNO_3 + 1 M KOH	*Angew. Chem. Int. Ed.* 63, e202411068 (2024)
RuPt/Cu	--	-0.2	99.8	58.76	62	1.0 M KNO_3 + 1 M KOH	*Angew. Chem. Int. Ed.* 63, e202407810 (2024)
Co_3O_4/Cu-N-C	-0.71 50% iR	-0.8 50% iR	97.7	92.46	20	1.0 KNO_3 + 1 M KOH	*Nat. Commun.* 15, 3619 (2024)

SP-Fe1-Ti	--	-0.4	95.2	68.12	40	1.0 M $NaNO_3$ + 1 M KOH	*Nat. Commun.* 15, 88 (2024)
CoP-CNS	--	-1.03	90	52.63	123	1.0 M KNO_3 + 1 M KOH	*Nat. Commun.* 13, 7958 (2022)
Cu_1Co_5	--	0.075 80% iR	96.2	32.4	30	1.0 M KNO_3 + 1 M KOH	*ACS Catal.* 13, 10846-10854 (2023)
CoP NAs/CFC	--	-0.3	99.3	16.89	60	1.0 M $NaNO_3$ + 1 M NaOH	*Energy Environ. Sci.* 15, 760-770 (2022)
CuPc MDE	-0.6 85% iR	-0.32 85% iR	98.4	62.4	30	1.0 M $NaNO_3$ + 1 M NaOH	*Energy Environ. Sci.* 16, 2239-2246 (2023)
CuPd	--	-0.5	92.5	21.29	12	1.0 M KNO_3 + 1 M KOH	*Nat. Commun.* 13, 2338 (2022)
CuNi NPs/CF	-0.38	-0.48	97.03	94.57	12	0.71 M $NaNO_3$ + 1 M NaOH	*Energy Environ. Sci.* 16, 2991-3001 (2023)
Cu_1Co_1	-0.5	-0.5	96.15	78.77	20	0.5 M KNO_3 + 1 M KOH	*J. Am. Chem. Soc.* 146, 27417-27428 (2024)
Au skin-Au Cu_3	--	0.55	96	12.94	110	0.5 M KNO_3 + 1 M KOH	*Angew. Chem. Int. Ed.* 63, e202408758 (2024)
CoP@Co	--	-0.2 100% iR	96.7	17.88	5	0.5 M KNO_3 + 1 M KOH	*J. Am. Chem. Soc.* 146, 12976-12983 (2024)
Pd-Cl/Cu_2O	-0.5	-0.6	97.5	53.46	10	0.5 M KNO_3 + 1 M KOH	*Nat. Commun.* 15, 1264 (2024)
Ni/$Ni(OH)_2$	-0.53	-0.467	98.5	84.74	102	0.5 M KNO_3 + 1 M KOH	*Angew. Chem. Int. Ed.* 63, e202406750 (2024)
Cu(100)/(111)	--	-0.36 85% iR	95	18.39	700	0.2 M KNO_3 + 1 M KOH	*Angew. Chem. Int. Ed.* 62, e202303327 (2023)
$CuCo_2O_4$	-0.84	-0.8	96.8	114.9	22	0.2 M NO_X^- + 1 M NaOH	*Adv. Mater.* 35, 2303455 (2023)
Fe_2O_3/Fe-N-C	-0.86	-1.0	100.7	115.81	24	0.16 M KNO_3 + 1 M KOH	*Adv. Mater.* 36, 2401133 (2024)
P-Cu/$Co(OH)_2$	--	-0.4	97.04	42.63	12	0.1 M KNO_3 + 1 M KOH	*Adv. Mater.* 36, 2408680 (2024)

$Cu/\beta\text{-}Co(OH)_2$	-0.6	-0.5	97.7	66.42	30	0.1 M KNO_3 + 1 M KOH	*Adv. Energy Mater.* 14, 2402805 (2024)
$Ni(OH)_2/Ni$	--	-0.8	98.99	47.85	50	0.1 M KNO_3 + 1 M KOH	*Nat. Commun.* 15, 6675 (2024)
Cu_3N/GDY	--	-0.9	98.1	35.28	5	0.1 M KNO_3 + 1 M KOH	*J. Am. Chem. Soc.* 146, 14898-14904 (2024)
Cu_9S_5-SNWs	--	-0.3 90% iR	90.4	6.3	20	0.1 M KNO_3 + 1 M KOH	*Adv. Energy Mater.* 15, 2403354 (2025)
$Cu\text{-}N_4B_2$	--	-0.6 100% iR	98.2	68.63	30	0.1 M KNO_3 + 1 M KOH	*Energy Environ. Sci.* 17, 8360-8367 (2024)
$Fe\text{-}Ni_2P$@NF	-0.6	-0.8	96.1	90.8	132	0.1 M KNO_3 + 1 M KOH	*Angew. Chem. Int. Ed.* 64, e202415300 (2024)

Note: the FE_{NH_3} in the table represents the highest FE_{NH_3} observed for the catalyst, and the corresponding E and $yield_{NH3}$ align with the highest FE.

Comment 5. The enhanced NO_3RR performance of Co_6Ni_4 catalyst may be attributed to its larger electrochemically active area. To better understand the origin of the high NO_3RR performance of Co_6Ni_4, the intrinsic activity of Co_6Ni_4 catalyst should be investigated and compared with Co and Ni catalysts.

Response: We are grateful for your valuable comment. We tested the ECSA of catalysts via the commonly used ECSA sweep rate extrapolation method.

Comparing the ECSA-normalized NH_3 current density and NH_3 yield of the Co_6Ni_4, Ni, and Co catalysts (**Figures R4a and b**), it can be found that the Co_6Ni_4 catalyst exhibits enhanced intrinsic activity than the Ni catalyst. However, the intrinsic activity of the Co catalyst appears anomalous, which could be due to its severe construction. The ECSA values were derived from CV tests in the non-Faradaic region. During both the non-Faradaic potential window and subsequent NO_3RR reactions, Ni and Co_6Ni_4 show negligible reconstruction, ensuring the accuracy and comparability of their ECSA results. These findings align with their geometric-area-normalized NO_3RR performance. For the Co catalyst, the spontaneous reaction between Co and NO_3^- leads to $Co(OH)_2$ formation in non-Faradaic potential region. Additionally, the Co catalyst exhibited varying degrees of reconstruction under different applied potentials during NO_3RR process, which result in significant discrepancies between its actual ECSA and the ECSA measured in the non-Faradaic region. This discrepancy is more profound at

more negative potentials, at which the catalyst reconstruction is more severe. Consequently, the ECSA-normalized current density and yield cannot truly reflect the intrinsic catalytic activity.

In summary, the intrinsic activity of Co_6Ni_4 catalyst is higher than Ni catalyst, but it is currently unable to accurately compare the intrinsic activity of Co_6Ni_4 catalyst and Co catalyst. Due to the severe reconstruction behavior of the Co catalyst, we are currently unable to confirm its intrinsic activity through accurate measurement of its ECSA. Therefore, the higher current density and ammonia yield of Co_6Ni_4 catalyst compared to Co catalyst could be due to the larger ECSA and higher intrinsic activity of Co_6Ni_4 catalyst.

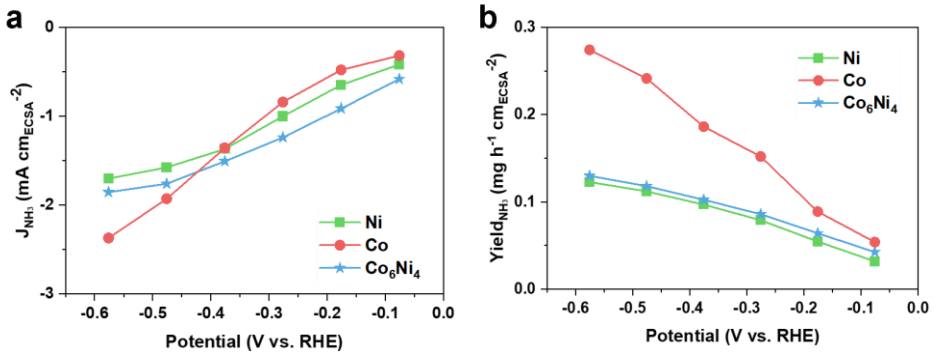

Figure R4. ECSA-normalized (a) current density and (b) yield rate towards NH_3 production for the Co_6Ni_4, Co, and Ni catalysts.

The ECSA of catalysts was estimated by the equation: $ECSA = \frac{C_{dl}}{C_s}$, where C_s = 60 μF cm^{-2} (*J. Am. Chem. Soc* 2025, 147, 12228-12238; *Nat. Commun*. 2022, 13, 7754).

Reviewer #2: This paper presents a well-executed and interesting study on the possible structure reconstruction phenomenon of Co-based catalysts toward electrocatalytic nitrate reduction reaction (NO_3RR). Co_6Ni_4 heterostructured materials as a model catalyst was developed, and suggested with high NO_3RR activity, even under industrially ampere current conditions. The improved performance and stable structure arise from the electron communication with Ni and Co domains in Co_6Ni_4, where the Ni domains transfer electrons to Co and prevent the accumulation of high-valence Co. The manuscript is well-structured, logically coherent, and presents a comprehensive combination of electrochemical analysis, in-situ/ex-situ material characterization to support the conclusions. The work is of high relevance to the field of nitrate reduction

reaction for ammonia production and will be valuable for both fundamental research and industrial applications. Therefore, I recommend acceptance after addressing the following issues:

Response: We sincerely appreciate your recognition and guidance on this work. Below are our detailed replies to each of your questions:

Comment 1. When deciphering the structure ordering within Co_6Ni_4 catalyst, author used the relative intensity of metal-metal scattering path to explain the atomic ordering of Co and Ni. Author should use this description with great caution, as the synchrotron radiation data does not sufficiently support the related conclusion. Otherwise, references must be cited in relevant part.

Response: We greatly appreciate your valuable suggestion. In EXAFS, the intensity of the R-space oscillations can serve as a parameter reflecting the degree of atomic ordering, coordination number, and dynamic disorder (atomic thermal vibrations). The EXAFS data in the manuscript show that the peak intensity of the Co-M bond in Co_6Ni_4 is lower than that of the Co-Co bond in Co foil (**Fig. 1i**), while the peak intensity of the Ni-M bond in Co_6Ni_4 is nearly the same as that of the Ni-Ni bond in Ni foil. For crystalline Co (hcp phase) and Ni (fcc phase), both of them have the same coordination number, hence the reduced peak intensity of Co-M bond in Co_6Ni_4 indicates that the reduced coordination number of Co suggests a decrease in atomic ordering - i.e., the presence of an amorphous phase. This conclusion is further supported by the XRD (**Supplementary Fig. 2**) and HR-TEM data (**Figure c**).
We have added two relevant references (*Phys. Rev. B* 1975, 11, 4836; *J. Am. Chem. Soc.* 2020, 142, 12306-12313) and made revision to ensure a more rigorous presentation in the manuscript.

Corresponding Revisions (Page 5):
Moreover, in the Co *K*-edge EXAFS spectrum of Co_6Ni_4 catalyst, the main peak at 2.18 Å can be ascribed to Co-Co coordination (**Fig. 1i**), while the peak intensity is obviously lower than that of Co foil, implying the lower atomic ordering of Co component in Co_6Ni_4.[43] Similarly, the main peak in the Ni K-edge EXAFS spectrum of Co_6Ni_4 catalyst (**Fig. 1j**), the main peak at 2.18 Å is assigned to Ni-Ni coordination and has almost the same intensity as that of Ni foil, indicating the high atomic ordering of Ni

component in Co_6Ni_4.[44]

43. Stern, E.A., Sayers, D.E. & Lytle, F.W. Extended x-ray-absorption fine-structure technique. III. Determination of physical parameters. *Phys. Rev. B* **11**, 4836-4846 (1975).
44. Su, H. et al. Dynamic Evolution of Solid–Liquid Electrochemical Interfaces over Single-Atom Active Sites. *J. Am. Chem. Soc.* **142**, 12306-12313 (2020).

Comment 2. The electron transfer Ni domains to Co was the key point to prevent the accumulation of high-valence Co, that was proved by XPS and XAS. This phenomenon was also associated with oxidative state increase on Ni site, and valence state of Co, which seems in contradictory of XAS result, as the metallic state dominate the Co_6Ni_4 compositions. More explanation shall provide on this part.

Response: We appreciate your critical comment. The EXAFS and wavelet transform results in the manuscript (Fig. 1i, j & Supplementary Fig. 8) indicate that Co and Ni elements in Co_6Ni_4 are in a metallic state, and metallic bonds are formed between them. The combined XAS (Fig. 1g, h) and XPS results (Supplementary Fig. 7) demonstrate electronic interactions between the Co and Ni domains in Co_6Ni_4. This interaction leads to a redistribution of electron density, where the electron cloud shifts toward Co, resulting in an electron-rich metallic state for Co and an electron-deficient for Ni This electron cloud shifts does not induce changes in the oxidation states of Co and Ni.
We have made corresponding revisions in the main text to clarify this point.

Corresponding Revisions (Page 5&6)

In the Co_6Ni_4 catalyst, the binding energy of Co^0 exhibits a shift of 0.2 eV to lower energy compared to that in Co catalyst, while the binding energy of Ni^0 displays a shift of 0.3 eV to higher energy compared to that in Ni catalyst, which suggests that there is a strong electronic interaction between Co and Ni in Co_6Ni_4 catalyst, resulting in the electron cloud center shifting towards Co.[37, 38]

The Ni K-edge XANES spectrum of Co_6Ni_4 resembles that of Ni foil but the absorption edge energy of Co_6Ni_4 is slightly higher than that of Ni foil (Fig. 1h), indicating the Ni domains in Co_6Ni_4 are in an electron-deficient state due to the shift of the electron cloud center towards Co.

Both the XAS and XPS results imply the electronic shift between Ni and Co domains.

Comment 3. The Co_6Ni_4 consisted of abundant amorphous and crystalline part, the exact role of those heterostructure was not well illustrated for the structure-activity relationship.

Response: We sincerely appreciate your insightful comment. To investigate the influence of amorphous phase or amorphous/crystalline interface on the NO_3RR performance, we synthesized the high-crystallinity Co catalyst (Hc-Co). TEM and SAED results demonstrate its high crystallinity (Fig. R5a-d). The Co catalyst in the manuscript has low crystallinity (containing amorphous phase), thus it is denoted as Lc-Co in the subsequent discussion.

The NO_3RR performance evaluation reveals that the Lc-Co exhibits a significantly positive shift in the onset potential compared to the Hc-Co, indicating enhanced NO_3^- adsorption facilitated by the amorphous phase, which aligns with its superior current response (Fig. R6a). The Hc-Co and Lc-Co catalysts shows comparable FE_{NH_3} (Fig. R6b), and the Lc-Co catalyst exhibiting marginally higher FE values only at -0.076 V and -0.176 V. This suggests that the amorphous phase exerts minimal impact on FE_{NH_3}. The ammonia yield of Lc-Co catalyst is higher than that of Hc-Co (Fig. R6c), consistent with its enhanced reduction current in Fig. R6a.

It is worth noting that, the pure Co catalyst and the Co component in in Co_6Ni_4 catalyst both have very poor crystallinity, which eliminates the effect of crystallinity and ensures valid performance comparison and mechanistic analysis of NO_3RR in this work. Therefore, in our work, we focus on the effect of catalyst composition instead of crystallinity. Nevertheless, the effect of amorphous phase or amorphous/crystalline interface on the NO_3RR performance deserves more systematic study and we will study it further in the future work.

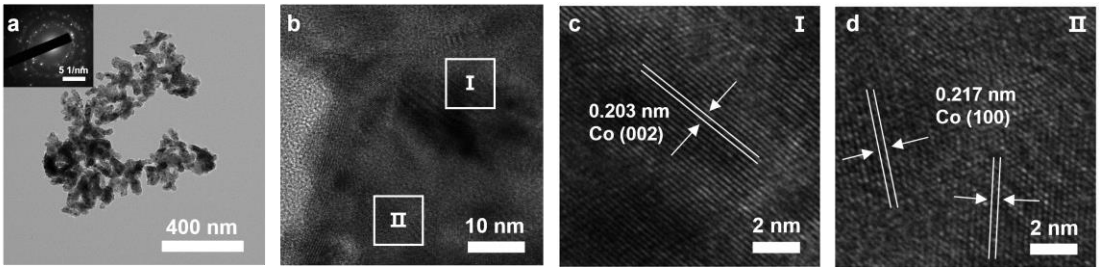

Figure R5. (a) TEM image and SAED pattern, (b-d) HR-TEM images of hcp-Co. Figures (d) and (e) correspond to regions I and II in figure (c), respectively.

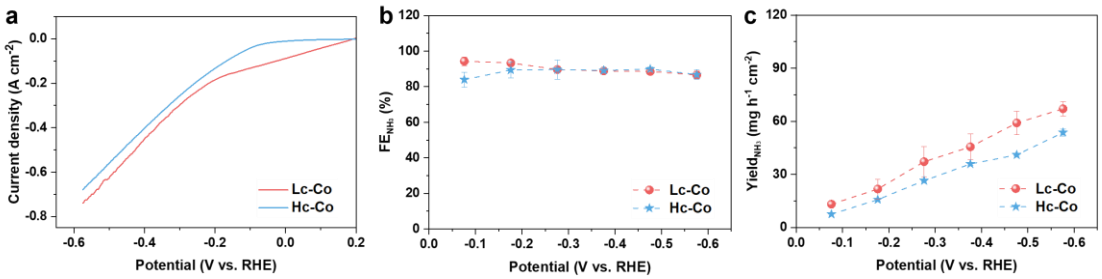

Figure R6. (a) LSV curves, (b) FE , and (c) yield rate of NH_3 of Lc-Co catalyst and Hc-Co catalyst.

Synthesis of high-crystallinity Co: Firstly, we prepared $Co(OH)_2$ using an electrodeposition method. The electrode selection and pretreatment of carbon paper followed the same procedures as described in the manuscript. The deposition electrolyte consisted of 30 mL of 0.5 M $Co(NO_3)_2$ aqueous solution, and electrodeposition was carried out at a constant current density of 10 mA cm^{-2} for 600 s. After deposition, the catalyst was thoroughly rinsed with pure water and dried in an oven at 60 °C to obtain $Co(OH)_2$. Subsequently, the $Co(OH)_2$ was annealed in a mixed Ar/H_2 (5%) atmosphere at 400 °C for 3 h, with a heating rate of 5 °C min^{-1}. The hcp-Co catalyst with high crystallinity was obtained after natural cooling.

Comment 4. How does the interaction between Ni and Co domains in Co_6Ni_4? Without any bond bridge within them, the electron transfer remains impossible. More concise discussion have to include for a better understanding of current work.

Response: Thanks for your valuable suggestion. The metallic nature of Co_6Ni_4 has been confirmed by XRD, TEM, and XAS characterizations (Supplementary Fig. 2 & Fig. 1a-d, g-h). and the EXAFS and wavelet transform analyses (Fig. 1i-j & Supplementary Fig. 8) demonstrate the formation of metallic bonds between Co and Ni. Although no conventional bridging bonds are observed, the delocalized nature of metallic bonds facilitates dynamic rearrangement of interfacial electron clouds (Fig. R7). This results in a shift of the electron cloud center toward Co (rendering it electron-enriched), while Ni becomes electron-deficient due to the migration of the electron cloud center (Fig. 5a). Theoretical calculations align consistently with XAS and XPS experimental results.

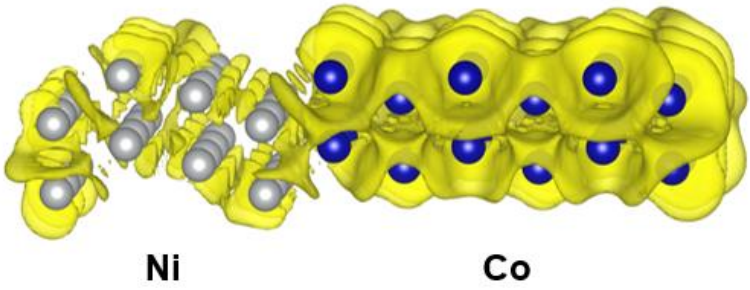

Figure R7. The electron localization distribution function of Co_6Ni_4. The yellow regions represent the electron cloud distribution.

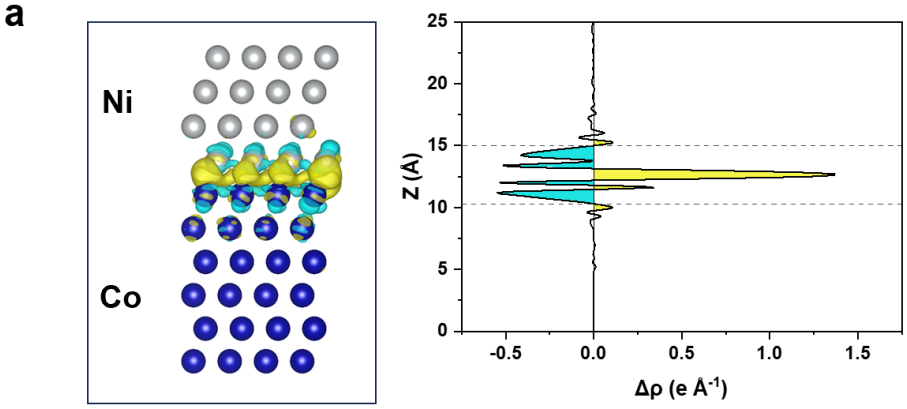

Figure 5. Theoretical calculation analysis. (a) Charge density difference and averaged electron density discrepancy for Co_6Ni_4 heterostructure interfaces.

Corresponding Revisions (Page 15)

By calculating the charge density, it is evident that electronic shift occurs at the Co/Ni interface of Co_6Ni_4, supporting our XAS and XPS analyses. Due to the delocalized nature of metallic bonds, the interfacial electron clouds undergo dynamic rearrangement. This ultimately leads to a shift of the electron cloud center towards Co, rendering it in an electron-enriched state, while Ni becomes electron-deficient (Fig. 5a).

Reviewer #3: In this study, the authors synthesized a series of CoxNiy heterostructured catalysts to investigate the reconstruction behavior of metallic Co during NO3RR. By combining operando XAS, in-situ Raman spectroscopy, and other characterization methods, they identified that the oxidation state evolution of Co arises from an imbalance between the catalyst's electron transfer capacity and the electron demand for adsorbed NO3- reduction. The Co6Ni4 catalyst achieves a high FE and high yield rate for NH3 production, as well as excellent stability. This work elucidates the origin of metallic Co reconstruction during NO3RR and proposes rational regulation strategies, offering critical insights for future catalyst design. The findings are impactful, and I

recommend it for publication after a minor revision.

Response: We are deeply grateful for your endorsement of our research efforts. Below are point-by-point responses to your inquiries:

Comment 1. The introduction states that NO_3RR typically exhibits higher NH_3 yield in alkaline environments compared to neutral conditions. Does this trend hold for Co_6Ni_4? A direct comparison of NH_3 FE and yield in neutral vs. alkaline electrolytes would clarify this claim.

Response: Thanks for your valuable question. Following the same methodology as in the manuscript, we evaluated the NO_3RR performance of Co_6Ni_4 in a neutral electrolyte (0.5 M K_2SO_4) and compare it with 1 M KOH. LSV curves show that the current density in 0.5 M K_2SO_4 is significantly lower than that in 1 M KOH , suggesting lower catalytic activity (Fig. R8a). Within the tested potential range, the Co_6Ni_4 catalyst exhibits a high FE_{NH_3} and NH_3 yield rate in the neutral environment increases as the applied potential becomes more negative, reaching a maximum FE_{NH_3} of 95.50% (Fig. R8b) and maximum yield rate of 58.43 mg h^{-1} cm^{-2} at a very negative potential of -0.876 V (Fig. R8c). At -0.476 V, the ammonia yield rate in the neutral environment is only 15.79 mg h^{-1} cm^{-2}, which is lower than that in the alkaline environment (93.55 mg h^{-1} cm^{-2}). These results indicate that the NO_3RR performance of Co_6Ni_4 in the neutral environment (pH = 7) is significantly inferior to that in the alkaline environment (pH = 14).

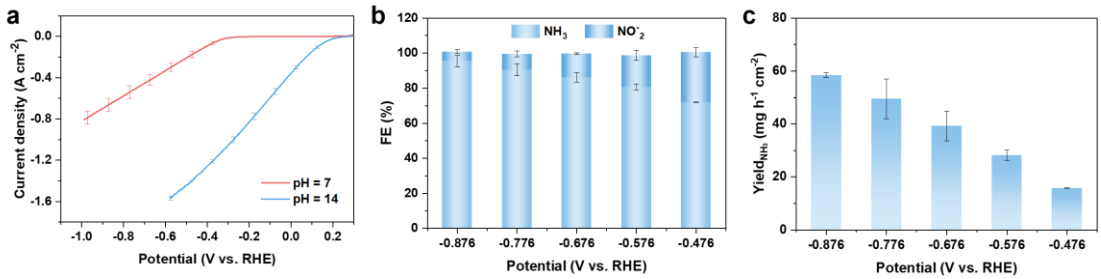

Figure R8. (a) LSV curves of Co_6Ni_4 for NO_3RR under neutral and alkaline conditions. (b) Corresponding FE and NH_3 yield rate at pH = 7.

Comment 2. In Figure S11, the current density in the first cycle is notably lower than in subsequent cycles. What causes this discrepancy?

Response: We appreciate your rigorous review. For the stability test, the Co_6Ni_4

catalyst was not pre-activated, which resulted in lower current density and FE in the first cycle. After the first-cycle test, the catalyst was activated and thus both the FE and current density returned to normal levels in the second cycle. We have incorporated corresponding explanations into the manuscript.

Corresponding Revision (Page 21)

Chronoamperometry (CA) was conducted at a constant potential for 1 h to detect the product. The catalyst was not activated prior to the stability test, and the electrolyte was replaced every 3 hours during the testing process.

Comment 3. At OCP, Co catalyst is oxidized to a higher valence state (Figures 3a and c), which suggests that the spontaneous reduction reaction of NO_3^- may occur. What are the products of this spontaneous NO_3^- reduction reaction? Does this interfere with NH_3 quantification or FE calculations?

Response: Thanks for your rigorous review and valuable questions. We monitored the primary products (NH_3 and NO_2^-) using UV-vis spectrophotometry after soaking the synthesized catalysts in a mixed solution of 1 M KOH + 0.3 M KNO_3 for 1 hour. The results indicate that a spontaneous reaction between Co and NO_3^- generates NH_3 and NO_2^-, whereas Co_6Ni_4 and Ni catalysts does not react spontaneously with NO_3^- (Fig. R9a and b). Subsequently, we analyzed the extent to which the spontaneous reaction in Co catalysts affects the quantitative NO_3RR product results. The NH_3 generated by the spontaneous reaction contributes less than 0.6% to the FE_{NH_3} of NO_3RR, and this influence further decreased at more negative potentials (Fig. R9c). Similarly, NO_2^- generated by the spontaneous reaction contributes less than 0.2% to the $FE_{NO_2^-}$ of NO_3RR, and this contribution decreased at more negative potentials (Fig. R9c). The yield of NH_3 and NO_2^- during this 1-hour spontaneous reaction of Co catalyst is 0.02 mg and 0.94 mg, respectively (Fig. R9d).

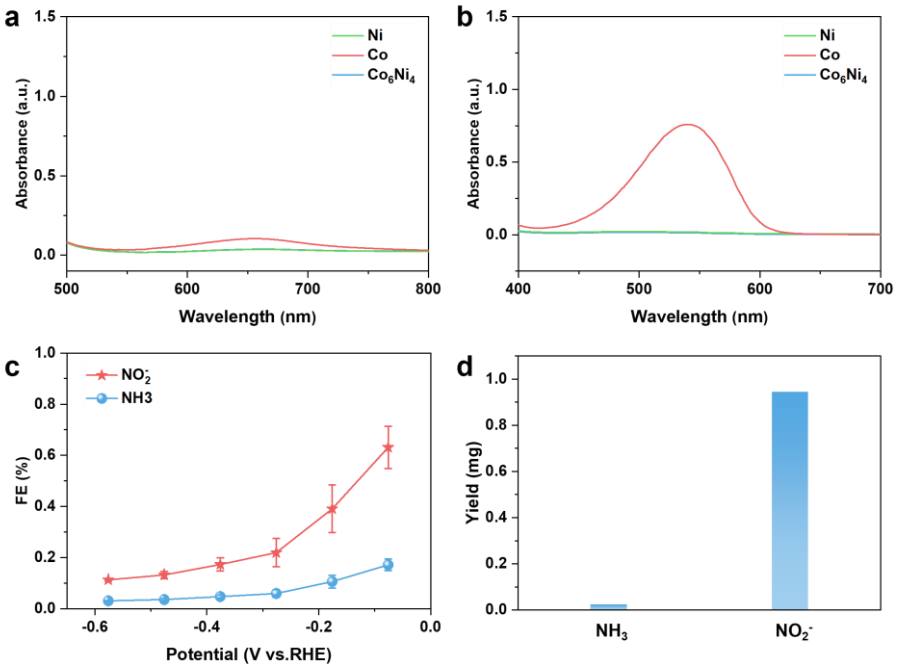

Figure R9. UV-vis absorption curves of (a) NH_3 and (b) NO_2^- produced by spontaneous reactions between Co_6Ni_4, Co, and Ni catalysts with NO_3^-. (c) FE and (d) yields of NH_3 and NO_2^- produced by spontaneous reaction between Co catalyst and NO_3^- under different NO_3RR potentials.

Comment 4. The MEA employs a proton-exchange membrane rather than an anion-exchange membrane. What is the rationale for this choice?

Response: Thank you for this critical question. We agree that in alkaline electrocatalytic reactions, such as alkaline electrocatalytic water splitting, anion-exchange membrane usually is the primary choice for ion transport. However, anion-exchange membrane also allows for NO_3^- transport in addition to OH^-. Therefore, during the MEA test, to maintain a steady NO_3^- concentration in the cathodic chamber and avoid any effect of NO_3^- on the anodic oxygen evolution reaction, we used proton exchange membrane to prevent NO_3^- diffusion (*Nat. Catal.* 2024, 7, 1032–1043).

Comment 5. Figure S13 and S14 reveal slight morphology change of Co_6Ni_4 after stability tests. The corresponding description in the manuscript needs to be revised.

Response: We appreciate your thorough review. The relevant descriptions in the manuscript have been revised accordingly.

Corresponding Revisions (Page 8)

The structure and morphology of Co_6Ni_4 remained largely unchanged after the cycling, except for the formation of corrosion-induced pores on the surface (**Supplementary Fig. 12-14**).

Comment 6. The manuscript repeatedly mentions that the performance of NO_3RR declines when the Co catalyst is oxidized to a higher valence state. Could the authors provide direct evidence to support this claim?

Response: We appreciate your insightful comment. We systematically compared the LSV curves and XRD patterns of the Co catalyst before and after NO_3RR activation. As shown in Fig. R10a, the current density of the Co catalyst exhibited a significant decrease after it was stabilized. XRD analysis revealed the substantial formation of $Co(OH)_2$ during the stabilization process (Fig. R10b), strongly suggesting that the accumulation of $Co(OH)_2$ is the primary factor responsible for the observed decline in current density.

To further validate this conclusion, we conducted comparative studies on $Co(OH)_2$ before and after NO_3RR activation. A marked increase in the current density of $Co(OH)_2$ was observed after it was stabilized (Fig. R10c). XRD results indicate partial conversion of $Co(OH)_2$ to metallic Co after stabilization (Fig. R10d). These findings reinforce that the NO_3RR activity of $Co(OH)_2$ is substantially lower than that of metallic Co, consistent with prior literature (*Adv. Sci.* 2021, 8, 2004523).

However, Co and $Co(OH)_2$ undergoes a dynamic interconversion during NO_3RR, thus it is hard to directly compare individual contributions from each phase.

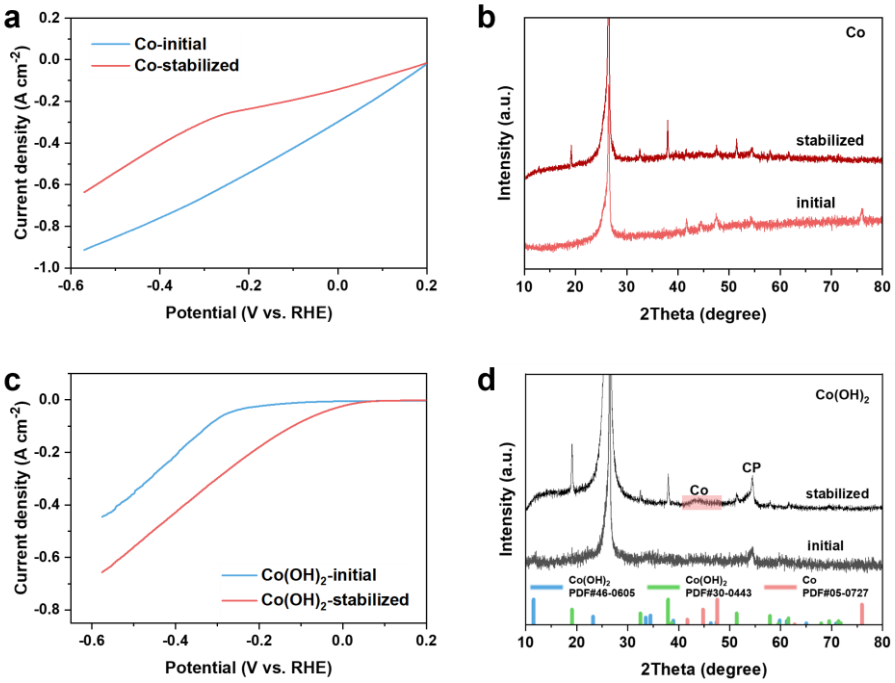

Figure R10. (a) LSV curves and (b) XRD patterns of Co catalyst before and after electrochemical oxidation. (c) LSV curves and (d) XRD patterns of $Co(OH)_2$ catalyst before and after stabilization.

Testing method for LSV curves: Multiple LSV scans were performed on the catalysts until the curve became stable. The first LSV scan and the LSV curve after stabilization were plotted

Synthesis of $Co(OH)_2$: We prepared $Co(OH)_2$ using an electrodeposition method. The electrode selection and pretreatment of carbon paper followed the same procedures as described in the manuscript. The deposition electrolyte consisted of 30 mL of 0.5 M $Co(NO_3)_2$ aqueous solution, and electrodeposition was carried out at a constant current density of 10 mA cm^{-2} for 600 s. After deposition, the catalyst was thoroughly rinsed with pure water and dried in an oven at 60 °C to obtain $Co(OH)_2$.